Liquid Crystals
Publication details, including instructions for authors and subscription information:
http://www.informaworld.com/smpp/title~content=t713926090

Liquid crystalline side chain methacrylic azo containing polymers

C. M. González-Henríquez[a]; E. A. Soto-Bustamante[a]; D. A. Waceols-Gordillo[a]; W. Haase[b]
[a] Universidad de Chile, Facultad de Ciencias Químicas y Farmacéuticas, Santiago 1, Chile [b] Technische Universität Darmstadt, Physikalische Chemie I, Petersenstr. 20, Germany

Online publication date: 05 November 2010

To cite this Article González-Henríquez, C. M. , Soto-Bustamante, E. A. , Waceols-Gordillo, D. A. and Haase, W.(2009) 'Liquid crystalline side chain methacrylic azo containing polymers', Liquid Crystals, 36: 5, 541 — 547
To link to this Article: DOI: 10.1080/02678290903045643
URL: http://dx.doi.org/10.1080/02678290903045643

Liquid Crystals,
Vol. 36, No. 5, May 2009, 541–547

Taylor & Francis
Taylor & Francis Group

Liquid crystalline side chain methacrylic azo containing polymers

C.M. González-Henríquez[a]*, E.A. Soto-Bustamante[a], D.A. Waceols-Gordillo[a] and W. Haase[b]

[a]*Universidad de Chile, Facultad de Ciencias Químicas y Farmacéuticas, Olivos 1007, Casilla 233, Santiago 1, Chile;* [b]*Technische Universität Darmstadt, Physikalische Chemie I, Petersenstr. 20, 64289-Darmstadt, Germany*

(Received 22 December 2008; final form 15 May 2009)

This paper describes the synthesis and characterisation of methacrylic liquid crystalline side chain polymer containing azo group, with (PM6OAn) and without (PM6An) hydroxyl group. The characterisation was done by using a polarised light microscope (PLM), differential thermal analysis (DTA), and X-ray diffractometry. All compounds developed bilayer smectic phase, with a certain degree of interdigitation between the layers. Poly[{3-hydroxy-4-[(E)-(4-octyloxyphenyl)diazenyl]phenoxy}hexyl]-2-methyl-prop-2-enoate (PM6OA8) exhibits a smectic A phase, whereas the other polymers show a SmC phase. Pyroelectric investigations show only an antiferroelectric behaviour for poly [{3-hydroxy-4-[(E)-(4-dodecyloxyphenyl)diazenyl]phenoxy}hexyl]-2-methylprop-2-enoate (PM6OA12) and a paraelectric behaviour for PM6OA8, poly[{4-[(E)-(4-dodecyloxyphenyl)diazenyl]phenoxy}hexyl]-2-methylprop-2-enoate (PM6A12) and poly [{4-[(E)-(4-octyloxyphenyl) diazenyl] phenoxy} hexyl]-2-methylprop-2-enoate (PM6A8). Finally, the E-Z photoisomerisation of the chromophores in solution was probed to exist in PM6A12 and PM6A8.

Keywords: azo aromatic polymers; bilayer smectic phase; photoisomerisation

1. Introduction

Liquid crystalline polymers (LCPs) containing azobenzene group have been widely studied overall in the field of optical materials (*1–11*). Most of these studies were based on the change in the optical anisotropy of the molecules within the liquid crystalline system, a property that can be driven photochemically. They usually are influenced by external stimuli such as photo-irradiation, change of temperature or application of an electric field. The photochemical process of the E-Z isomerisation (*12*) can be reversed by selecting the appropriate wavelength of irradiation.

In this work, we report the synthesis and characterisation of methacrylic liquid crystalline side chain azo containing polymers Poly[{3-hydroxy-4-[(E)-(4-alkyloxyphenyl)diazenyl]phenoxy}hexyl]-2-methylprop-2-enoate (PM6OAn) or poly [{4-[(E)-(4-alkyloxyphenyl)diazenyl]phenoxy}hexyl]-2-methylprop-2-enoate (PM6An) (see Figure 1). The abbreviation used indicates the presence of a polymer (P), methacrylic-like (M), linked through a six methylene unit as spacer (6) to the aromatic group (A). The aromatic group consists of two phenyl rings linked through an azo group in *para* position, where the nearest phenyl ring to the spacer (PM6) remains with and without a hydroxyl group in *meta* position (R). The aromatic group possesses, in its *para* position, an alkoxy flying tail with an octyl and dodecyloxy unit (8 and 12), respectively. Figure 1 shows the general structure of the polymers.

Our polymeric compounds are characterised by ^{1}H-NMR and gel permeation chromatography (GPC). The liquid crystalline properties are studied by DTA and mesophases corroborated by X-ray. The electric behaviour of the composites was investigated using the pyroelectric technique. Finally, the E-Z isomerisations in the azo compounds are achieved by applying a specific wavelength to the materials.

2. Experimental

2.1 Apparatus used

The polymers synthesised were characterised by ^{1}H-NMR spectroscopy using a 300 MHz spectrometer (Bruker, WM 300). The weight, number, and z-average molecular weight $\overline{M_w}$, $\overline{M_n}$, $\overline{M_z}$, the polydispersity index (*PDI*) and intrinsic viscosity (η) for the polymers were determined by GPC using a Waters 600 Controller microflow pump, with a Waters 410 Differential Refractometer as detector. A styragel HT4 (Waters) column, with tetrahydrofuran HPLC graded as eluent with a flow rate of 0.3 ml min^{-1} was used. The material used for calibration was polymethylmethacrylate (PMMA) as primary standard of known molecular weight ranging from $\overline{M_w}$ 5050 to 280,000 (WAT 035707 and WAT 035706).

The phase transition temperatures for the investigated polymers were determined using a differential thermal analyser (Mettler, FP90 DTA) with 0.1 K of accuracy. A polarising microscope (Leica, DLMP), equipped with a heating stage (HS-1, Instec) was used for temperature-dependent investigations of liquid crystal textures. A video camera (Panasonic,

*Corresponding author. Email: carmengh@ciq.uchile.cl

ISSN 0267-8292 print/ISSN 1366-5855 online

DOI: 10.1080/02678290903045643
http://www.informaworld.com

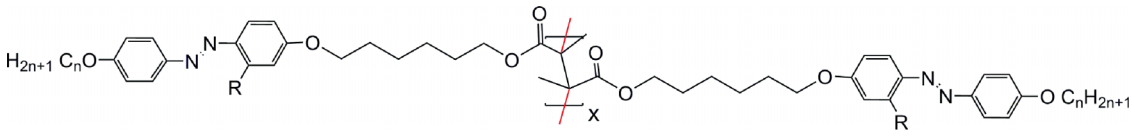

Figure 1. Polymers with R = H, n = 12 (PM6A12); R = H, n = 8 (PM6A8); R = OH, n = 12 (PM6OA12); R = OH, n = 8 (PM6OA8).

WVCP414P), installed on the polarising microscope, was coupled with a video capture card (Miro DC-30) that allowed real-time capture and image saving. The samples were supported between glass plates.

X-ray measurements were carried out using CuKα radiation; the samples were contained in 0.8-mm glass capillaries (Lindemann) and held in a copper block. The precise data for aligned samples in the small angle region were obtained by focusing a horizontal two-circle X-ray diffractometer (STOE STADI 2) with a linear position-sensitive detector for data collection. The temperature was stabilised within the range of 30°C to 170°C at ±0.1 K during the measurements.

For obtaining the pyroelectric signal (γ) of the polymers, the samples were confined in cells of 8 μm thickness at the isotropic phase for capillarity. The cells were placed inside a temperature-controlled thermal oven (Linkam THMSE 600) that allows a temperature control ranging from 0.1°C min^{-1} up to 20°C min^{-1}. To achieve low temperatures, an external cooling system (temperature-regulated cooler Linkam CI93 and Linkam LND) was used. The temperature variation pulses were applied to the samples using modulated light from a semiconductor laser (λ = 685 nm, P = 27 mW, modulation capability from DC to 5 MHz) fed by a 5DC volts power supply. The modulation frequency is provided by the lock-in amplifier at 70 Hz (EG&G Model T260 DSP); an oscilloscope (Hewlett Packard 54600A, with 2 channel 100 MHz) was used to corroborate in real time the evolution of the pyroelectric signal. The pyroelectric response from poled samples was measured as a sine voltage with the lock-in amplifier. To carry out the poling process, an external DC supply was used, constructed using standard 9-V batteries connected in series. The obtained data were acquired with a computer connected to the lock-in amplifier, and the data were further processed by appropriate software. The hysteresis loop was obtained using the same technique by following the pyroelectric signal developed for a sample at a constant temperature.

The UV-Vis spectra in THF solution were recorded using an ATI Unicam UV/Vis Spectrometer UV3. The light source for photo-irradiation was a 450 W meium pressure mercury lamp (Model B 100 AP) and a commercial dichroic lamp of 50 W for E-Z isomerisation. The wavelength was chosen at 360 nm for E→Z and 450 nm for Z→E isomerisation. In the first case, a bandwidth filter with two specific wavelengths at 366 nm and 746 nm (50.27% and 9.47% transmittance) was used. In the second case, a Vis-filter was used, with a cut-off at 392 nm (80–89% transmittance).

2.2 *Polymerisation process of azo-containing monomers*

The monomeric molecules were synthesised using well known methods described (*13*). The corresponding polymers were prepared using a typical methodology already described in (*14–16*), which can be summarised as follows. The monomers (0.5 g) were dissolved in dry toluene (4 ml). The reaction mixture was introduced into a Pyrex glass vial under nitrogen atmosphere. Afterwards, 2,2′-azobis-isobutyronitrile (AIBN) was added as radical initiator (*17*). The vial was degassed with nitrogen, sealed, and the reaction mixture was heated for 48 h to 60°C. The concentrated reaction mixture was directly poured into an excess of acetone to eliminate the excess of non-reacting monomer. The polymer formed was filtered off and cleaned successively by refluxing the solid in acetone and drying it overnight at 50°C under vacuum.

The polymer parameters were assessed by GPC and the values are summarised in Table 1. The structures of the polymers were determined by ^{1}H-NMR spectroscopy. The following is the ^{1}H-NMR for PM6OA12 and PM6A12: Poly[{3-hydroxy-4-[(E)-(4-dodecyloxyphenyl)diazenyl]phenoxy}hexyl]-2-methylprop-2-enoate (PM6OA12) ^{1}H-NMR ($CDCl_3$) δ ppm: 13.45 (s, 1H, OH-Arom-);7.58 (d, 2H, N=N-ArH), 7.51 (d, 1H -O-Ar(OH)-H-N=N-), 6.79 (d, 2H, -O-ArH-N=N-), (6.39 dd 1H and 6.26 d 1H, -O-2H-Ar(OH)-N=N), 3.80 (m,

Table 1. Molecular weight characterisation of polymer liquid crystals used in this study.

Polymer	$\overline{M_n}$	$\overline{M_w}$	$\overline{M_z}$	*PDI*	n_w
PM6OA8	16.677	56.119	108.125	3.36	110
PM6OA12	13.241	46.746	101.907	3.53	82
PM6A8	12.491	42.571	96.631	3.41	86
PM6A12	17.242	64.199	119.549	3.72	116

6H,-CH_2-O-Ar; CO_2-CH_2-); 1.66–1.17 (m, 28H, -CH_2-),0.79 (t, 3H, -CH_3-). Yield: 50%.

Poly[{4-[(E)-(4-dodecyloxyphenyl)diazenyl]phenoxy}-hexyl]-2-methylprop-2-enoate (PM6A12) ^{1}H-NMR ($CDCl_3$) δ ppm: 7.69 (d, 4H, N=N-ArH), 6.82 (dd, 4H, -O-ArH-N=N-), 3.80 (m, 6H,-CH_2-O-Ar; CO_2-CH_2-), 1.66–1.18 (m, 28H, -CH_2-),0.79 (t,3H, -CH_3-). Yield: 40%.

2.3 Gel permeation chromatography

Table 1 summarises the molecular weight characterisation of the studied samples. No traces of monomer or oligomer fractions in the samples were detected in the chromatograms. The molecular weight relationship between different molecular weights was as expected: $\overline{M_z} > \overline{M_w} > \overline{M_n}$. All the molecular weights of polymers fall between 40,000 and 65,000 D approximately. This fact, together with a quite reasonable dispersion index ($PDI = \overline{M_w}/\overline{M_n}$) ranging from 3.36 to 3.72, reflects the polymeric nature of the freshly polymerised samples, with a polymerisation degree n_w in an interval from 85 and 120.

3. Results and discussion

3.1 Polarised light microscopy

The polarised light microscopy confirmed two types of mesophase present in the studied polymers, by cooling and heating. Figure 2(a) shows the texture of a smectic C phase at 161.1°C for PM6A12, also seen in samples of PM6A8 and PM6OA12, where it is possible to see the presence of singularities possessing four brushes with $s = \pm 1$. This texture is called schlieren and the brushes appear smoother and somehow washed out for the smectic C phase. A different texture is observed for the polymer PM6OA8, which developed a smectic A phase. This topology consists of smectic layers arranged basically perpendicular to the substrate of plane producing an ellipse, showing a perfect system of Dupin cyclides (see Figure 2(b)). Both mesophases are observed in all the liquid crystalline ranges of each polymer sample.

3.2 Differential thermal analysis

Table 2 summarises the phase transition temperatures for the polymers, taken as the maximum temperature in the DTA enthalpic peaks, as well as the corresponding glass transition temperature (T_g). The thermograms showed one event by cooling and also by heating, related to the change from the liquid crystalline to the isotropic state and *vice versa*. In case of PM6OA12, two peaks can be observed, one of them related to the transition to the isotropic state as well, and the second one at lower temperature, related to the crystallisation process. All the polymers show a T_g that is typical for this class of compounds, between 71°C and 94°C. It is important to note that the glass transition temperature is a thermodynamic parameter, and thus parametrically depends on the cooling rate. These data are obtained from the first scanning by heating, using a heating rate of 4°C min^{-1}, where T_g was taken as the half-devitrification temperature.

Below T_g, the polymers take on a fragile conformation, they become rigid and brittle, and can crack and shatter under stress. If we increase the temperature over T_g, a greater flexibility appears, showing the liquid crystalline character of the samples typical of a soft material.

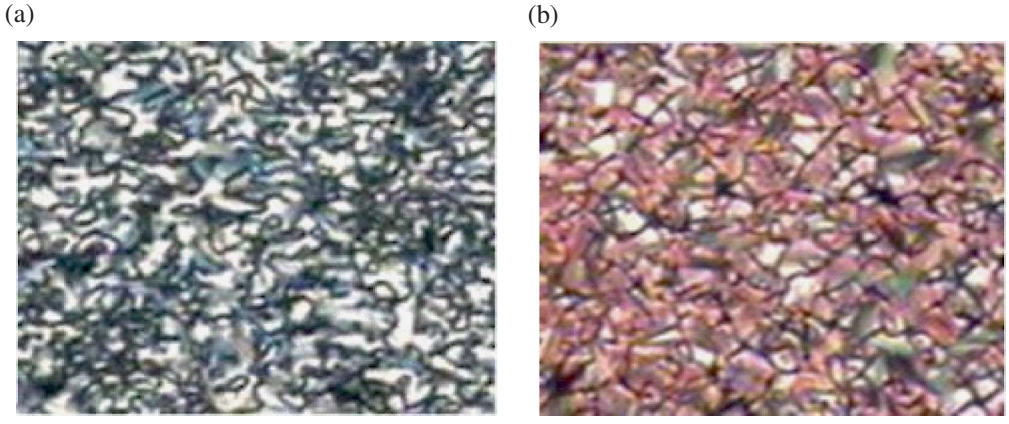

Figure 2. Representative liquid-crystalline textures. (a) Smectic C phase (PM6A12, T = 161.1°C); (b) smectic A phase (PM6OA8, T = 130°C).

Table 2. Heating and cooling scans obtained by differential thermal analysis (DTA) for the investigated polymers.

Sample	Heating	Cooling
PM6A8	G-79.8-SmC-164.1°C(34.2 J g^{-1})-I	I-159.3°C(–28.0 J g^{-1})-SmC-n.d.-C
PM6A12	G-88.2-SmC-175.3°C(11.8 J g^{-1})-I	I-171.2°C(–12.1 J g^{-1})-SmC-n.d.-C
PM6OA8	G-88.0-SmA-151.3°C(7.4 J g^{-1})-I	I-149.3°C(–6.0 J g^{-1})-SmA-n.d.-C
PM6OA12	G-93.3-SmC-178.3°C(9.0 J g^{-1})-I	I-173.7°C(–8.3 J g^{-1})-SmC n.d.-C

n.d., not determined.

3.3 X-ray studies

X-ray measurements were carried out in polymers PM6OA12, PM6A12 and PM6A8. Attempts to characterise the polymer PM6OA8 by X-ray diffraction were unsuccessful due to a smaller amount of sample. The X-ray diffraction patterns for PM6A8, PM6A12 and PM6OA12 show a series of reflections corresponding to d_{001}, d_{002} and in the case of PM6A8, to d_{003} also. The presence of these peaks, together with the temperature dependence of the interlayer distance, supports the existence of a smectic C phase in the samples. The first reflections, corresponding to the interlayer periodicity, significantly exceed the length, L, of the side chains, where d/L is in the range 1.62 to 1.45, depending on temperature. This implies a bilayer arrangement of side-chain mesogenic units in smectic layers, with a certain degree of interdigitation at the interface. The broad peaks in the wide angle region permit us to calculate the average intermolecular distances, D, within the smectic layers (Table 3). Thus molecular packing within the smectic layers must be considered as liquid-like. The PM6OA12 polymer, which has a hydroxyl group in *meta* position of the aromatic core, shows a diffraction peak in the wide angle region broader than in the case of the PM6A12 polymer. This can be understood as a more liquid-like behaviour of the side chains accompanied by an increase of the distance D due to lateral substitution.

The experimental interlayer spacings (d), taken from X-ray measurements, are displayed in Figure 3. All polymers show a smectic C phase between 180°C and 80°C. At low temperature only a smooth change of interlayer distance is observed, which could be related to a decrease in the movement or arrangement of the molecules due to a decrease in the viscosity of the system. This change must be related to the glass transition temperature of the system, observed by DTA in the first scanning by heating and not detected by PLM. Interestingly, the interlayer distance for polymer with side chains without OH group in the aromatic core (PM6A12) shows a larger value when compared with the corresponding PM6OA12 sample. This result is in good agreement with our previous studies on Schiff Base compounds (*18*), where the layer periodicity for PM6B8 without OH group was also larger than for PM6R8, the homologous compound with lateral hydroxyl group, 54 Å against 51 Å respectively.

The explanation of this must be in the molecular conformation of the side chains, which allows the hydrogen bonding between the hydroxyl and the nitrogen in the azo linkage of the aromatic core. In the case of molecules without hydroxyl group no interactions with the aromatic core through hydrogen bonding are allowed and the side chains adopt a more relaxed structure, with a small tilt angle and therefore a long interlayer distance.

Table 3. Experimental interlayer distances d, average intermolecular distances in the layers D and tilt angles β for the mesophases.

Polymer, T = 140°C	d(001)	D	Angle β
PM6A12	60.12	4.59	39.1
PM6A8	54.14	4.37	36.5
PM6OA12	57.80	4.43 (90)	41.8

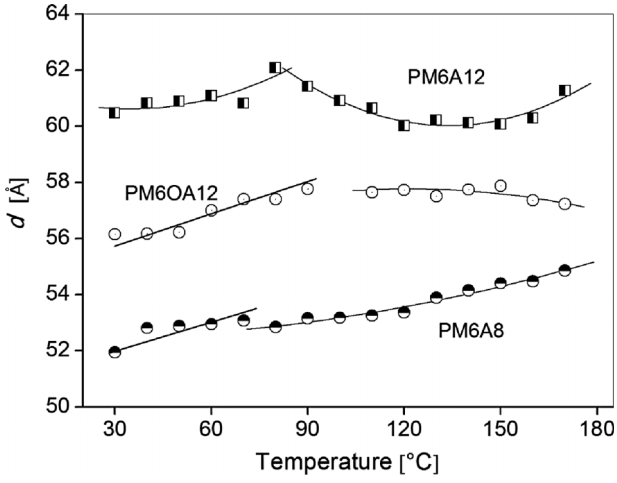

Figure 3. Temperature dependence of the interlayer distance under cooling for the polymers.

3.4 Pyroelectric measurements

Preliminary results on pyroelectric measurements were carried out using the modulation pyroelectric technique described above. The poling process was carried out from the isotropic state until room temperature through the liquid crystalline phase. The bias strength was 103 V, around 10 V μm^{-1} at 20°C. The external field was removed and the samples were connected to the lock-in amplifier and heated to 4°C above the isotropic state.

The values of the pyroelectric coefficient (γ) for the polymers were obtained using a pulse pyroelectric technique (*14*,*15*) according to the simple equation (T_I is the transition temperature to the isotropic phase):

$$Ps(T) = \int_{T_1}^{T} \gamma(T) dT. \qquad (1)$$

The correct scale for (γ) and *Ps* was introduced by comparison of the pyroelectric response at a certain temperature with the value measured for a known ferroelectric substance, in this case FLC-397 (*19*). The temperature dependence of the pyroelectric signals for PM6OA12 is shown in Figure 4(a).

In the case of PM6A8, PM6A12 and PM6OA8, the typical repolarisation loop in coordinates' bias voltage-pyroresponse shows near linear field dependence that is characteristic for linear dielectrics with field-induced polarisation. For the first two samples the explanation can be found in the absence of hydrogen bonding, due to the absence of OH groups. In the case of PM6OA8, the only explanation arises from the presence of an orthogonal interdigitated SmA phase, which in the case of liquid crystals is due to symmetry considerations, and is a well-known para-electric.

Opposite to that, PM6OA12 developed a pyroelectric signal from the glassy state inside the liquid crystalline phase. As can be seen in Figure 4(a) the pyroelectric response decreases in the glassy state. Also the phase transitions are shifted to lower temperatures. This fact may be indicative of a decrease in the value of the viscosity of the sample. The calculated macroscopic polarisation using Equation (1), from the obtained pyroelectric signal, shows moderate values of polarisation, estimated to be 65 nC cm^{-2} when compared with our previous samples. In the case of our Schiff bases values for composites consisting of polymers and their corresponding monomers (*14–16*) were reported as high as 400 nC cm^{-2}. The samples show typical antiferroelectric loops corresponding to three stable states: one with zero polarisation in the absence of the field, and two states with the macroscopic polarisation orientated along two possible directions of the external field (see Figure 4(b)).

3.5 Photoresponsive properties

Once again, differences were noticed depending on the aromatic substitution, which can be easily understood since ortho hydroxy substituted azobenzols do not undergo E-Z isomerisation, but tautomerisation due to proton transfer to the corresponding hydrazone, which also is responsible for the luminescence process observed in these compounds (*20*) Attempts to obtain E-Z isomerisation were completely unsuccessful under our experimental conditions.

The phenomenon of E-Z photoisomerisation was studied in tetrahydrofurane (THF) solutions of PM6A12 and PM6A8 not possessing OH group.

Figure 5 shows the UV-Vis spectra of LC-azopolymer dissolved in THF. After 20 s of UV light irradiation, the high intensity absorption peak of azobenzene in the E form centred at 359 nm (π–π^* transition)

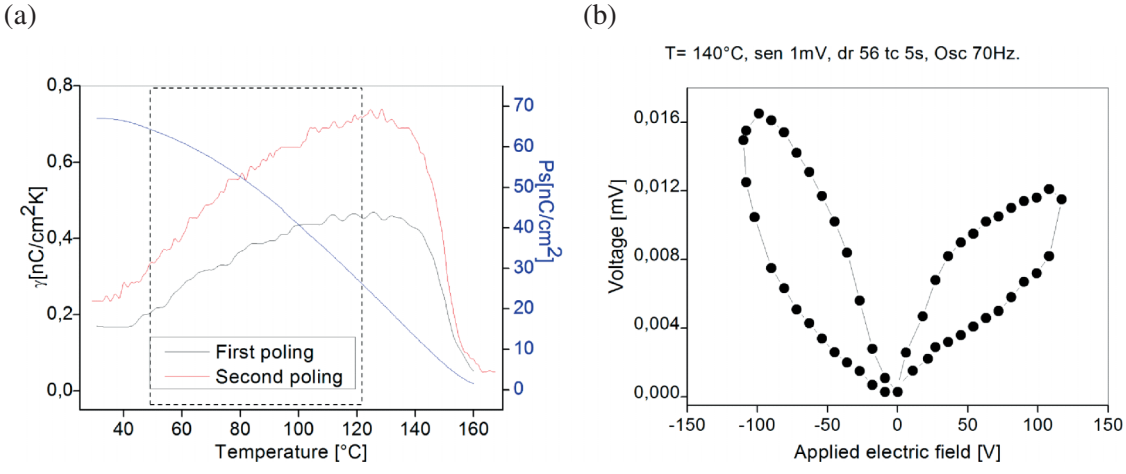

Figure 4. (a) Pyroelectric response; (b) hysteresis loop for the polymer PM6OA12 at 140°C.

almost disappears, and is replaced by a low intensity absorption peak of azobenzene in the Z conformation near 450 nm (n–π*). The UV irradiation caused both the diminution in absorbance around 359 nm and an increase in the absorbance to the 450 nm, indicating the E→Z photo-isomerisation.

Visible light at 450 nm induced Z→E photo-isomerisation of the azobenzene. When the polymer is irradiated for 1 h, the quantity of side chains that relax back through this process is smaller (see Figure 5(b), $t = 60$ min, $A = 0.50$) than the amount of molecules that initially transit from E→Z conformation due to UV light exposition (see Figure 5(a), $t = 0$ min, $A = 0.61$). Further irradiation with 450 nm does not change the absorption peak of E azobenzene.

After reaching the limit of Z absorbance, around 1 h, we left the compound overnight in darkness, without irradiation. A slight increase in the absorbance of the E configuration, when compared with the initial one, was observed, which may be related with the loss of the solvent.

Both absorption spectra show two isosbestic point, at 319 nm and 428 nm, where two absorping molecules are present in equilibrium. The gradual decrease in absorbance at longer wavelengths may be an evidence for cyclo-addition or isomerisation reactions (*21*).

The ratio E/Z of the azo compounds produced for the UV and Vis irradiation was determined by means of Equations (2) (*22*) and (3). To estimate the percentage of Z azobenzene at the photostationary state, Equation (2) was used. Here A_0 and A_z correspond to the absorbance at 360 nm before irradiation and at any time during irradiation, respectively. When the conversion reaches about 100%, we can estimate the irradiation time for the full E→Z isomerisation:

$$\%Z = 100(A_0 - A_Z)/A_0. \quad (2)$$

The percentage of E azobenzene at the photostationary state, produced for the UV-Vis irradiation, was determined by means of Equation (3), where A_0 and A_E are the absorbance at 359 nm before irradiation and at any time during irradiation with 450 nm wavelength, respectively:

$$\%E = 100(A_E)/A_0. \quad (3)$$

Within the first seconds a very fast change of the chromophores is observed, the Z configuration taking place, reaching a maximum of 95% for the PM6A12 and 99% of conversion for the PM6A8. The PM6A12 reached the Z configuration faster than the PM6A8 polymer, which is reflected in the percentage after 30 s of irradiation, which must be related with a high flexibility of the side chains in the solvent due to the longer aliphatic chain. The feedback isomerisation is rather slow, due perhaps to less quantum efficiency of the visible lamp, compared with the UV-Vis one.

4. Conclusion

Polymers PM6OA12, PM6A12 and PM6A8 show a smectic C phase within the whole liquid crystalline temperature range, whereas polymer PM6OA8 presents a smectic A phase. All these data are corroborated by DTA, PLM and X-ray diffractometry. The layer arrangement in these materials is strongly affected by the lateral OH group substitution. They adopt a less relaxed structure exhibiting a small angle and therefore a big interlayer distance that can be explained by intramolecular interaction or hydrogen bridges. In the opposite case, when no OH group is

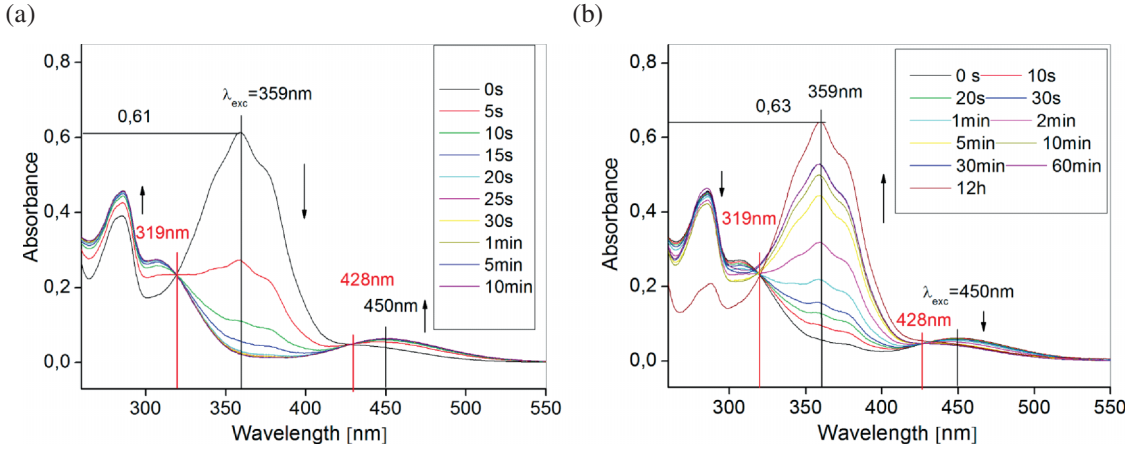

Figure 5. (Colour online). Changes in the absorption spectra for the PM6A12: (a) E→Z; (b) Z→E photo-isomerisation.

present, the tilt angle in the mesophase is more pronounced, reflected in shorter interlayer distance.

Polymer PM6OA12 presents an antiferroelectric behaviour, expressed in the developed hysteresis loop, where molecules adopt an opposite tilt direction for alternate smectic layer, with an unwounded state of polarisation at zero field.

In the case of the other materials, in polymer PM6OA8, the presence of the orthogonal SmA phase does not promote polar mesophase, whereas in PM6A12 and PM6A8, the absence of lateral OH group is responsible for the para-electric behaviour. Both effects have been carefully described in our earlier publications (*13–15*, *18*). The lateral hydroxyl groups also affect the photo-isomerisation process as could be expected, and no E-Z photo-isomerisation was allowed in PM6OA8 or in PM6OA12. On the other hand, PM6A12 and PM6A8 were photo-isomerised at the usual irradiation wavelengths of 366 and 450 nm. The isomerisation process take place in timeframes comparable to the literature, that is between 20 s and 1 min. The feedback isomerisation is rather slow, at around 1 h.

Acknowledgements

C.M. González-Henríquez acknowledges a Scholarship from Conicyt and E.A. Soto-Bustamante is grateful for financial support from Project FONDECYT 2007 Nr. 1071059 and Merck Chile S.A.

References

(1) Eich, M.; Wendorff, J.H.; Reck, B.; Ringsdorf, H. *Makromol. Chem. Rapid Commun*. **1987**, *8*, 59–63.
(2) Ikeda, T.; Tsutsumi, O. *Science* **1995**, *268*, 1873–1875.
(3) Sung, J-H.; Hirano, S.; Tsutsumi, O.; Kanazawa, A.; Shiono, T.; Ikeda, T. *Chem. Mater.* **2002**, *14*, 385–391.
(4) Ruslim, C.; Ichimura, K. *Adv. Mater*. **2001**, *13*, 37–39.
(5) Ruslim, C.; Ichimura, K. *Adv. Mater*. **2001**, *13*, 641–643.
(6) Shibaev, V.P.; Kostromin, S.G.; Plate, N.A.; Ivanov, S.A.; Vetro, V. Yu.; Yakovlev, I.A. *Polym. Commun*. **1983**, *24*, 364–365.
(7) Cole, H.J.; Simon, R. *Polymer* **1985**, *26*, 1801–1806.
(8) Ikeda, T.; Horiuchi, S.; Karanjit, D.B.; Kurihara, S.; Tazuke, S. *Macromolecules* **1990**, *23*, 36–42.
(9) Ikeda, T.; Horiuchi, S.; Karanjit, D.B.; Kurihara, S.; Tazuke, S. *Macromolecules* **1990**, *23*, 42–48.
(10) Ikeda, T.; Kurihara, S.; Karanjit, D.B.; Tazuke, S. *Macromolecules* **1990**, *23*, 3938–3943.
(11) Sasaki, T.; Ikeda, T.; Ichimura, K. *Macromolecules* **1992**, *25*, 3807–3811.
(12) Serak, S.V.; Arikainen, E.O.; Gleeson, H.F.; Grozhik, V.A.; Guillou, J.P.; Usova, N.A. *Liq. Cryst.* **2002**, *29*, 19–26.
(13) Soto Bustamante, E.A.; Yablonskii, S.V.; Beresnev, L.A.; Blinov, L.M.; Haase, W.; Dultz, W.; Galyametdinov, Yu.G. *Methode zur Herstellung von polymeren pyroelektrischen und piezoelektrischen Elementen*, German Patent: No. 195 47 934.3, 20 Dic 1995, DE 195 47 934 A1, 26 Jun 1997; European Patent: EP 0 780 914 A1 25 Jun 1997; Japan Patent: JP 237921/907 09 Sep 1997; US Patent: US 5 833 833, 10 Nov 1998.
(14) Soto Bustamante, E.A.; Yablonskii, S.V.; Ostrovskii, B.I.; Beresnev, L.A.; Blinov, L.M.; Haase, W. *Chem. Phys. Lett*. **1996**, *260*, 447–452.
(15) Soto Bustamante, E.A.; Yablonskii, S.V.; Ostrovskii, B.I.; Beresnev, L.A.; Blinov, L.M.; Haase, W. *Liq. Cryst.* **1996**, 21, 829–839.
(16) Soto-Bustamante, E.A.; Saldaño-Hurtado, D.; Vergara-Toloza, R.O.; Navarrete-Encina, P.A. *Liq. Cryst.* **2000**, *30*, 17–22.
(17) Ingold, K.U. In *Free Radical*, Kochi, J.K., Ed.; Wiley: New York, 1973; Chap. 1.
(18) Ostrovskii, B.I.; Soto Bustamante, E.A.; Sulianov, S.N.; Galyamedtinov, Yu.; Haase, W. *Mol. Mat.* **1996**, *6*, 171–188.
(19) Hiller, S.; Beresnev, L.A.; Pikin, S.A.; Haase, W. *Ferroelectrics* **1996**, *180*, 153–163.
(20) Nurmukhametov, R.N.; Shigorin, D.N.; Kozlov, Yu.I; Puchkov, V.A. *Opt. Spectrosc*. **1961**, *11*, 602–612.
(21) Choi, K.-S.; Kim, H.-W.; Kim, Y.-B.; Kim, J.-D. *Liq. Cryst*. **2004**, *31*, 639–647.
(22) Cui, L.; Zhao, Y.; Yavrian, A.; Galstian, T. *Macromolecules* **2003**, *36*, 8246–8252.